Available online at www.sciencedirect.com
SCIENCE DIRECT
ELSEVIER
Journal of the European Ceramic Society 26 (2006) 1385–1391
ECERS
www.elsevier.com/locate/jeurceramsoc

Quantitative analysis of lattice distortion in $Ba(Zn_{1/3}Ta_{2/3})O_3$ microwave dielectric ceramics with added B_2O_3 using Raman spectroscopy

C.J. Lee [a,1], G. Pezzotti [a], Shin H. Kang [b], Deug J. Kim [b,*], Kug Sun Hong [c]

[a] *Ceramic Physics Laboratory, Department of Materials, Kyoto Institute of Technology, Sakyo-ku, Matsugasaki, 606-8585 Kyoto, Japan*
[b] *Department of Materials Engineering, SungKyunKwan University, Suwon 440-746, South Korea*
[c] *School of Materials Science & Engineering, College of Engineering, Seoul National University, Seoul, South Korea*

Received 25 November 2004; received in revised form 7 February 2005; accepted 19 February 2005
Available online 17 May 2005

Abstract

$A(B'_{1/3}B''_{2/3})O_3$ complex perovskites are primary candidates for microwave dielectric materials because of their high dielectric constants, very low dielectric losses, and low temperature coefficients of resonant frequency. In this study, the ordering and lattice distortion related to the cation ordering in the $Ba(Zn_{1/3}Ta_{2/3})O_3$–B_2O_3 system were investigated using X-ray diffraction and Raman spectroscopy. The residual stress caused by the lattice distortion associated with ordering was explained in terms of the Raman line shift. The 1:2 ordered structure of the pure BZT ceramics was replaced by a 1:1 ordered structure at 1650 °C. The addition of B_2O_3 improved the ordering in the BZT ceramics, and the degree of 1:2 ordering increased with increasing B_2O_3 content. The Raman lines of the 1:1 ordered structure were shifted towards lower wavenumbers, as compared to the disordered structures, which proves that compressive stresses were stored in the 1:1 ordered ceramics. On the other hand, in the case of the 1:2 ordered structure, the Raman lines shifted towards higher wavenumbers and the ceramics were subjected to tensile stress. The maximum $Q \times f$ value was obtained from the 1:1 ordered pure BZT ceramic sintered at 1650 °C. The $Q \times f$ value decreased with increasing B_2O_3 content, in spite of the highly ordered 1:2 structure.

Keyword: BZT; Perovskites; Dielectric properties; Grain growth; Sintering; $Ba(Zn)TaO_3$

1. Introduction

$A(B'_{1/3}B''_{2/3})O_3$ complex perovskites, where B′ = Zn or Mg and B″ = Nb or Ta, are primary candidates for microwave dielectric materials, because of their high dielectric constants, low dielectric losses, and low temperature coefficients of resonant frequency.[1,2] Among them, $Ba(Zn_{1/3}Ta_{2/3})O_3$ (BZT), which has a high ε_r value of greater than 25, a near-zero temperature coefficient and a high quality factor, Q, at microwave frequency, is widely used in wireless communications systems.[3–6]

$Ba(Zn_{1/3}Ta_{2/3})O_3$ is a disorder–order, complex perovskite ceramic and it is well known that the Zn^{2+} and Ta^{5+} ions individual (1 1 1) crystallographic planes of the perovskite subcell.[7,8] In BZT, the B-site cations are stoichiometrically ordered in the form of a hexagonal cell, with one Zn^{2+} layer and two Ta^{5+} layers repeated along the ⟨1 1 1⟩ direction of the parent perovskite cubic cell. This ordering is a matter of considerable interest, because it is believed to be closely related to the high quality factor of BZT in microwave communications.[4,6,9]

The highest Q values are achieved in compounds with 1:2 ordering, and are obtained by annealing the ceramics for long times at above 1400 °C.[9] It was suggested that the high Q value of BZT could be attributed to the volatilization of ZnO after extended high-temperature sintering.[6] On the other hand, Tamura et al.[5] showed that the enhancement of the Q

* Corresponding author.
E-mail address: kimdj@skku.ac.kr (D.J. Kim).
[1] Present address: Samsung Electro-mechanics Co., Ltd., Maetan-3-dong, Paldal-gu, Suwon, South Korea.

0955-2219/$ – see front matter © 2005 Elsevier Ltd. All rights reserved.
doi:10.1016/j.jeurceramsoc.2005.02.014

value was not related to cation ordering. A recent paper explained that the high Q value observed in the BZT–$BaZrO_3$ system was related to the stabilization of the grain boundary and the lowering of the free energy of the anti-phase boundaries.[10]

Many studies of BZT have been conducted using powder X-ray diffraction (XRD) and TEM, in order to explore its ordering structure. Recently, the effects of ordering on the Raman spectra of $Ba(Mg_{1/3}Ta_{2/3})O_3$ (BMT) and BZT were reported.[11,12] An ideal cubic perovskite structure with the space group of $Pm3m$ symmetry, in which the B-site cations are randomly distributed, does not show any Raman active mode, whereas a 1:1 ordered perovskite structure with a space group of $Fm3m$ symmetry allows four strong Raman lines. Siny et al. found these four Raman lines in BMT and attributed them to domains of 1:1 ordering. The 1:2 ordered perovskite structure based on $P\bar{3}ml$ symmetry gives nine Raman active modes.[13–15]

Furthermore, Zn and Ta ordering simultaneously causes lattice distortion, due to the expansion of the parent cubic cell in the direction of the ordered (1 1 1) planes.[16] Therefore, the ideal value for the hexagonal structure was found to deviate from the c/a of $(3/2)^{1/2}$. In addition, from a structural point of view, the anti-phase boundary (APB) in the trigonal 1:2 structure produces considerable elastic strain. Kawashima et al.[4] observed splitting in the (4 2 2) and (2 2 6) reflections, caused by the lattice distortion resulting from Zn–Ta ordering. While the relationship between a high value of the quality factor, Q, and cation ordering has been extensively studied, the effect of distortion arising from cation ordering has been overlooked.

In this study, B_2O_3 was added to BZT ceramics, in order to improve their sinterability. The effect of the lattice distortion, which is associated with the cation ordering in the $Ba(Zn_{1/3}Ta_{2/3})O_3$ system, was investigated using XRD and Raman spectroscopy. The lattice distortion associated with ordering was able to be explained in terms of residual stress on the basis of the observed Raman line shifts. In addition, the correlation between the ordering, residual stress and dielectric loss is also discussed.

2. Experimental procedure

2.1. Specimen preparation

Reagent-grade (purity >99.9%) $BaCO_3$, Ta_2O_5, ZnO and B_2O_3 were used as the raw material powders. Stoichiometric amounts of the raw powders were weighed and then mixed in deionized water with ZrO_2 balls for 12 h. The mixture was then calcined at a temperature of 1100 °C for 2 h. The calcined powder was ball milled again with 0–3 wt.% B_2O_3 in deionized water with ZrO_2 balls for 24 h. After it was dried, binder was added to the powder, which was then pressed into disks and sintered at 1100 to 1650 °C for 2 h. Sintering was carried out in a platinum crucible and the specimens subsequently allowed to cool in the furnace. The sintered specimens were ground and polished, and examined by X-ray diffractometry (XRD) using Cu Kα radiation and by scanning electron microscopy (SEM). The density was measured using Archimedes' method. The dielectric loss tangent was measured in a cylindrical resonator cavity made of copper at 10 GHz with a Hewlett Packard gratitude HP 8720C Network Analyzer.

2.2. Raman spectroscopy analysis

The spectra were measured with a Raman microprobe spectrometer (ISA, T-64000, Jobin-Ivon/Horiba Group, Tokyo, Japan) at room temperature. The 488 nm line of an Ar-ion laser with a power of 200 mW was used as the excitation source. An optical microscope was used both to focus the laser on the sample and to collect its scattered signal. The scattered frequencies were analyzed using a triple-monochromator equipped with a charge-coupled device (CCD) camera. The highest lateral resolution achievable for the laser beam focused on the sample was about 1 μm. The recorded spectra were analyzed with commercial software (SpectraCal, Galactic Industries) and the wavenumber shifts obtained from the differences between the peak centers for the calcined powder and the sintered samples.

3. Results

3.1. Microstructure

Fig. 1 shows the variation of the relative density as a function of the sintering temperature in the pure and 0.1 wt.% B_2O_3-added BZT samples; sintering was always performed for 2 h. It was very difficult to sinter the pure BZT without additives. The relative density of pure BZT reached about 95% at 1650 °C after a holding time of 2 h. On the other hand, the relative density of the 0.1 wt.% B_2O_3 added BZT sample reached about 97.5% even at 1400 °C, which is attributed to

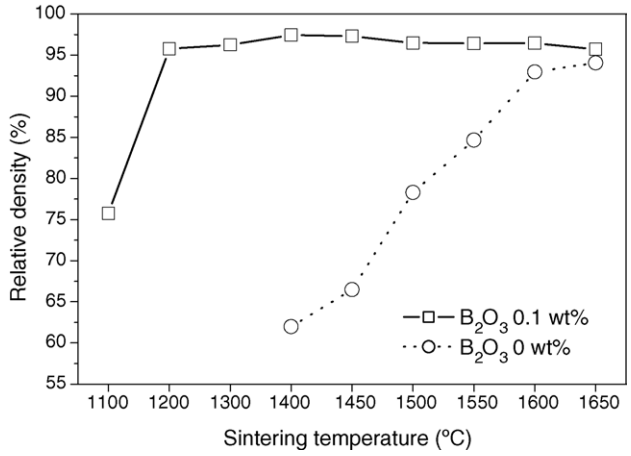

Fig. 1. Densities of the BZT ceramics as a function of the sintering temperature.

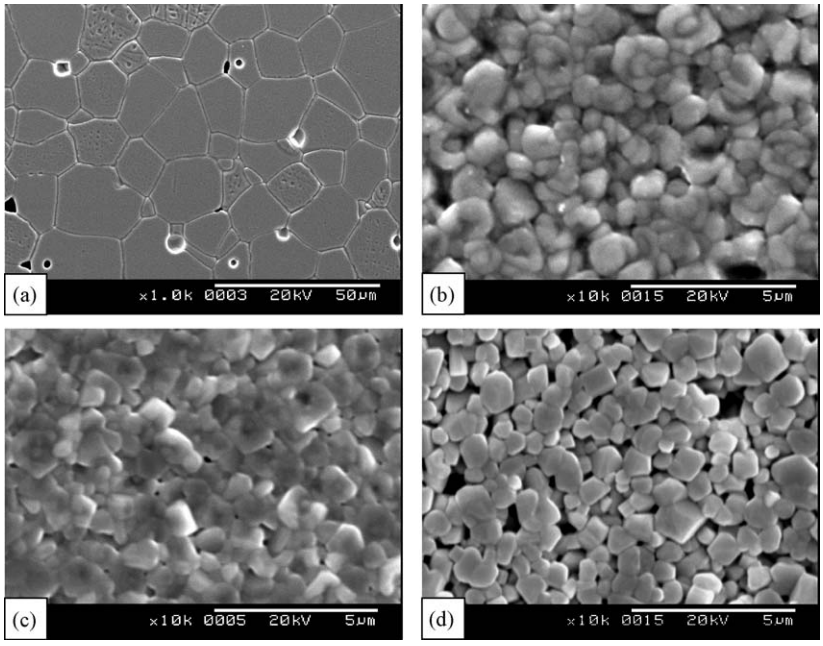

Fig. 2. SEM micrographs of the BZT–B_2O_3 ceramics. Part (a) is the pure BZT sample sintered at 1650 °C for 2 h. Parts (b)–(d) are the samples with 0.1 wt.%, 0.3 wt.% and 3 wt.% B_2O_3, respectively, sintered at 1400 °C for 2 h.

the low melting point of B_2O_3 (≈420 °C) and to the increase in the sinterability afforded by the presence of a liquid phase. The slight decrease in the sinterability at temperatures above 1400 °C is due to pore formation caused by over-firing.

The microstructures of the pure and B_2O_3-added BZT samples, sintered at 1650 °C and 1400 °C, respectively, for 2 h are shown in Fig. 2. The grain size of the pure BZT sample sintered at 1650 °C was larger than 20 um, and a porous microstructure was observed, due to the evaporation of ZnO during the sintering process (Fig. 2(a)). The grain size of the B_2O_3-added BZT sample after sintering at 1400 °C was in the sub-micrometer range, however, no remarkable variation in the microstructure depending on the amount of B_2O_3 added was found (Fig. 2(b)–(d)). Kawashima et al.[4] reported a slow rate of grain growth between 1350 and 1600 °C and a dramatic variation in grain size at temperatures above 1600 °C. Although the grain growth mechanism was not clarified and no evidence of liquid phase sintering was given in their report, Reaney et al.[17] observed grain rounding, which is characteristic of the presence of a liquid phase at the grain boundaries. Therefore, it is considered that the large grain size of the sample sintered at 1650 °C is related to the formation of a liquid phase at high temperature (above 1600 °C).

3.2. XRD

Fig. 3 shows the XRD patterns of the samples shown in Fig. 2 in the range of 10–80°. All of the diffraction peaks were indexed based on the 1:2 ordered hexagonal superstructure. The (1 0 0) peak, which arises from the 1:2 ordering of Zn^{2+} and Ta^{5+}, is known to be one of the strongest reflection. However, no superstructure reflections associated with 1:2 ordering were detected in the pure BZT ceramics sintered at 1650 °C, which could be associated with a transition in the ordering. On the other hand, the samples sintered at 1400 °C with B_2O_3 contents of 0.1, 0.3 and 3 wt.% exhibited superstructure reflections from 17.5°, and the intensity of the (1 0 0) peak increased with increasing B_2O_3 content. It has previously been reported based on the XRD patterns, that second phases of $Ba_3B_2O_6$ and $TaBO_4$ exist in the samples with 0.3 and 3 wt.% B_2O_3. Therefore, it is assumed that the addition of B_2O_3 improved the 1:2 ordering of the BZT ceramics. Further details about the ordering will be discussed in the next section, in the light of the results of the Raman analysis.

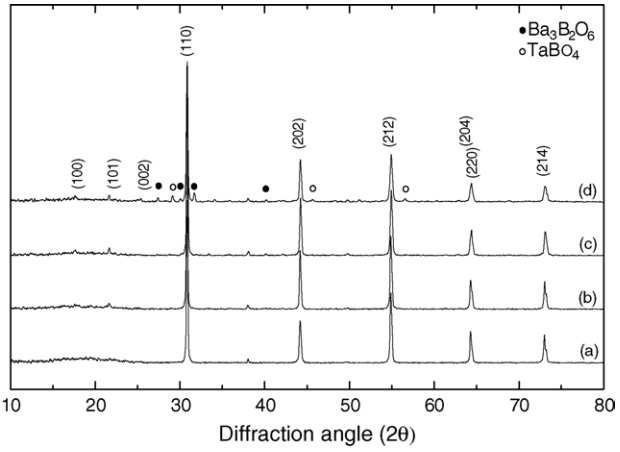

Fig. 3. X-ray diffraction patterns for the BZT–B_2O_3 ceramics. (a) Pure BZT sintered at 1650 °C for 2 h; (b)–(d) samples with 0.1 wt.%, 0.3 wt.% and 3 wt.% B_2O_3, respectively, sintered at 1400 °C for 2 h.

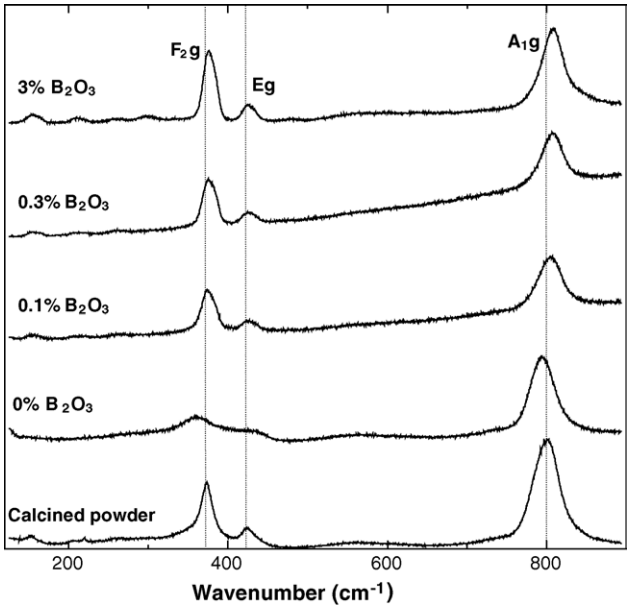

Fig. 4. Raman spectra for calcined powder and BZT–B_2O_3 ceramics. (a) Calcined powder; (b) pure BZT sintered at 1650 °C for 2 h; (c)–(e) samples with 0.1 wt.%, 0.3 wt.% and 3 wt.% B_2O_3, respectively, sintered at 1400 °C for 2 h.

3.3. Raman spectra

From the viewpoint of the lattice vibration, a BZT crystal with an ideal cubic perovskite structure (space group of *Pm*3*m* symmetry, in which the B-site cations are randomly distributed) does not show any Raman active mode. However, a 1:1 ordered perovskite with a space group of Fm3m symmetry allows for four strong Raman lines:[14]

$$\Gamma = A_{1g}[O] + E_{2g}[O] + 2F_{2g}[A + O], \quad (1)$$

where the square brackets shows the ions involved in a particular normal vibration mode. On the other hand, the 1:2 ordered perovskite structure based on *P*3*m*1 symmetry gives nine Raman active modes:[15]

$$\Gamma = 4A_{1g}[A, B'', O] + 5E_g[A, B'', O]. \quad (2)$$

The Raman spectra of the calcined powder and the four sintered samples described in Fig. 2 are given in Fig. 4. The strongest Raman line was indexed based on the 1:1 ordered perovskite with the space group of *Fm*3*m* symmetry, in which another F_{2g} line also existed at around 101 cm^{-1} (not shown in this figure). It was expected that the mixed powder calcined at 1100 °C for 2 h would have a cubic perovskite structure and, thus, show no Raman lines. However, contrary to our expectations, four strong and some extra Raman lines were observed. Siny et al.[12] showed that no considerable difference in shape, position or intensity can be found between the Raman spectra of ceramics and crystal fibers; the former exhibiting 1:2 ordering, while the latter remain disordered. Raman lines in a disordered structure are attributed to the loss of both transitional and inverse symmetries, due to disordering in the B-site cations. In the case of the pure BZT sample sintered at 1650 °C for 2 h, the Raman lines of F_{2g} and A_{1g}, which originate from the tortional vibration modes of the B-site ions are broadened and move towards a lower wavenumber, as compared with the Raman lines of the calcined powder. However, the three extra lines in the range of 150–300 cm^{-1}, which are the characteristic feature of the 1:2 ordered complex perovskite, were not observed. On the other hand, the Raman lines of F_{2g} and A_{1g} in the samples sintered at 1400 °C for 2 h with 0.1, 0.3 and 3 wt.% B_2O_3 contents were sharp and moved towards a higher wavenumber, as compared with those of the calcined powder; also, the characteristic lines of a 1:2 ordered structure appeared at around 156, 211 and 260 cm^{-1}. The intensity of the three extra Raman lines increased with increasing B_2O_3 content, as shown in Fig. 5(a). As shown in Fig. 5(b), the vibrational modes, F_{2g} and A_{1g}, shifted to a higher wavenumber, i.e. from 361 to 376.8 cm^{-1} and from 794.5 to 806.9 cm^{-1}, respectively, with increasing B_2O_3 content. From the results of the XRD and Raman analysis, it was concluded that the ad-

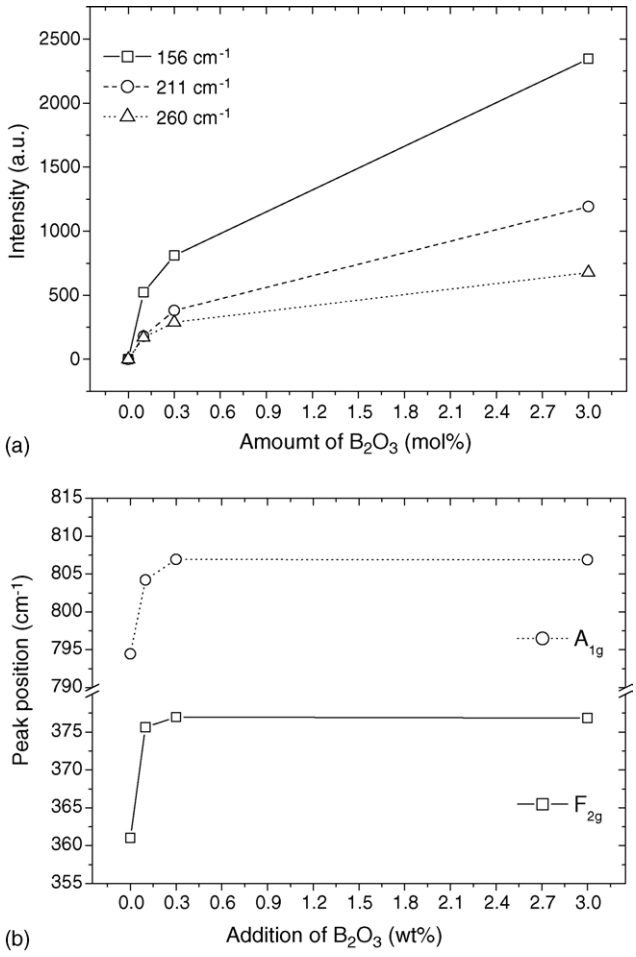

Fig. 5. Parts (a) and (b) are the intensity changes of the three extra Raman lines and the Raman shifts of the F_{2g} and A_{1g} modes as a function of the B_2O_3 content, respectively.

dition of B_2O_3 improved the ordering in the BZT ceramics, due to the Zn^{2+} and Ta^{5+} ions being able to easily rearrange their position in the B-site, because of the presence of Ba or Ta vacancies resulting from the formation of $Ba_3B_2O_6$ and $TaBO_4$ second phases. It is reasonable to assume that the sample sintered at 1650 °C for 2 h deviated from the 1:2 ordering, because no characteristic features of 1:2 ordering were found in either the XRD pattern or Raman spectra.

4. Discussion

In order to evaluate the relationship between the ordering and the quality factor, the appearance of superlattice peaks and the splitting of reflections related to the deviation of the c/a ratio from the ideal cubic perovskite structure were investigated.[4,6,9] Until recently, no attention was paid to the quantitative amount of distortion caused by ordering. Our results show that the shift in the Raman lines towards the left or right is associated with the ordering. In this section, we discuss the relationship between the shift of the Raman lines and the ordering.

If the B′ and B″ ions in the $A(B'_{1/3}B''_{2/3})O_3$ complex perovskites, which normally have a disordered structure, are rearranged to from a 1:1 or 1:2 ordered structure, the crystallographic structure is changed from cubic to face-centered cubic in the case of 1:1 ordering or trigonal in the case of 1:2 ordering. During this process, lattice distortion associated with ordering is produced, and it is this lattice distortion that is the origin of the shift in the Raman lines. This shift in the Raman lines can be explained in terms of the residual stress.

In a first-order approximation for a single-crystal whose principal applied stresses are exactly oriented along the crystalline axes, the stress dependence of a Raman band position is governed by the following tensorial expression:

$$\Delta\nu = \Pi_{ij}\sigma_{ij} \tag{3}$$

where $\Delta\nu$ is the wavenumber shift, σ_{ij} the stress tensor, and Π_{ij} is the matrix of the piezo-spectroscopic (PS) coefficients. However, in the case of polycrystalline samples with a randomly oriented stress tensor, Eq. (3) can only be applied with statistical significance, provided that a statistically meaningful number of microcrystals are probed during the measurement. The measured frequency shift, $\langle\Delta\nu\rangle$, usually obeys a linear relationship with the applied stress, independent of the nature of the stress:

$$\langle\Delta\nu\rangle = \Pi_{\mathrm{tr}}\langle\sigma\rangle \tag{4}$$

where Π_{tr} is the trace of the PS tensor and $\langle\sigma\rangle$ is the average stress value. When applying simple uniaxial stress to a polycrystalline body, the uniaxial piezo-spectroscopic coefficient, Π_{u} ($\equiv\Pi_{\mathrm{tr}}$), can be calculated from the peak-shift measurements using the phenomenological relation described by Eq. (4). This was the experimental procedure used here for measuring Π_{u} from the bulk BZT ceramics. The residual stresses were considered to be equi-triaxial in the first approximation, and were calculated based on a hydrostatic (and isotropic) piezo-spectroscopic coefficient, $\Pi_{\mathrm{h}} = 3\Pi_{\mathrm{u}}$.

The wavenumber used as the standard value for zero external stress was obtained by averaging about 50 spectra collected for a mixed powder calcined at 1100 °C for 2 h. Although it is difficult to conclude that the calcined powder has a completely disordered structure, it would be a mistake to affirm that the wavenumber obtained from the calcined powder represents the standard value for stress-free conditions, because of the low calcined temperature and short sintering time. The stress dependence of the Raman band of F_{2g} and A_{1g} was calibrated using the bulk BZT ceramics. A specially designed jig was used to apply an uniaxial compressive stress field to a specimen with dimensions of 2 mm × 3 mm × 1 mm. A compressive load well below the fracture stress threshold of the calibration specimen was applied and its magnitude could be precisely estimated by means of standard equations. Further details of the stress calibration procedure using the four-point bending method are given elsewhere.[18] The entire jig was placed under the optical microscope situated in the Raman microprobe device, and the Raman lines were recorded, while increasing the external compressive stress. The stress dependence of the F_{2g} and A_{1g} Raman lines are shown in Fig. 6(a) and (b), respectively. The uniaxial piezo-spectroscopic coefficients for the F_{2g} and A_{1g} lines were $\Pi_{\mathrm{u}} = 8.57 \pm 0.2$ and $7.43 \pm 0.2\ \mathrm{cm^{-1}\ GPa^{-1}}$, respectively.

Fig. 7 shows the stress caused by the lattice distortion for the samples without B_2O_3 sintered at 1650 °C and those with 0.1, 0.3 and 3 wt.% B_2O_3 sintered at 1400 °C, where the stress was obtained by scanning a 100 μm × 100 μm area with a step size of 2 μm and averaging the approximately 2500 spectra collected for each sample (laser spot size ≈1 μm). The stress was always compressive in nature in the pure BZT sample sintered at 1650 °C without B_2O_3: approximately 219 MPa for the F_{2g} mode and 478 MPa for the A_{1g} mode, while there was also tensile stress (maximum value of 140 MPa for the F_{2g} mode and 339 MPa for the A_{1g} mode) in the samples with B_2O_3 sintered at 1400 °C. The stress increased with increasing B_2O_3 content. From the viewpoint of the crystallographic structure, it is reasonable to conclude that compressive or tensile stress is produced when the crystallographic structure changes from cubic to face-centered cubic in the case of 1:1 ordering or trigonal in the case of 1:2 ordering, respectively. Therefore, it was concluded from the XRD results and the shift in the Raman lines (c.f. Figs. 3, 5 and 7) that the 1:2 ordering was replaced by 1:1 ordering in the sample sintered at 1650 °C for 2 h.

Fig. 8 illustrates the intensity changes in the F_{2g} and A_{1g} modes resulting from the addition of B_2O_3 as a function of the degree of dielectric loss ($Q \times f$). In this figure, 0, 0.1, 0.3 and 3 indicate the wt% of B_2O_3. The maximum value of $Q \times f$

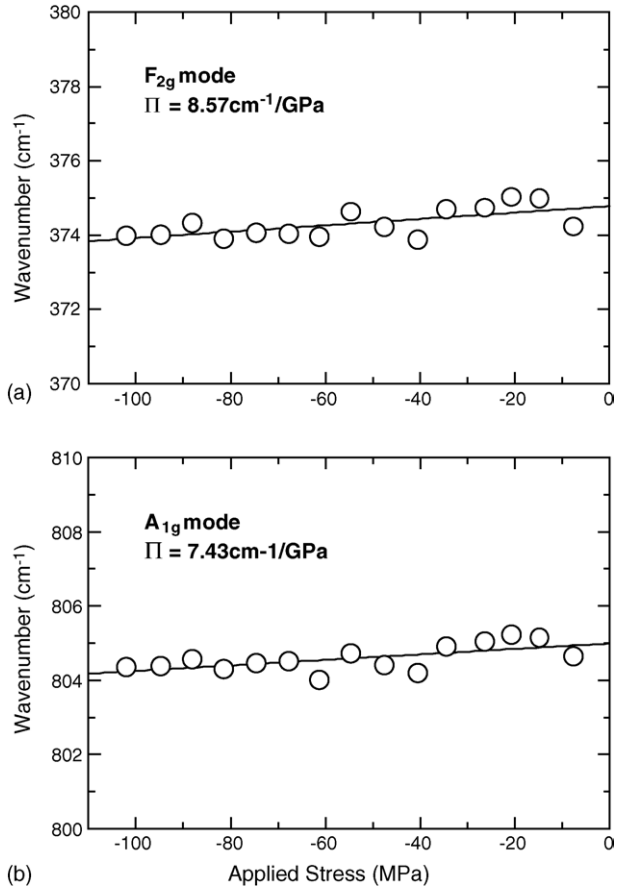

Fig. 6. Parts (a) and (b) are the stress dependence of the Raman lines of the F_{2g} and A_{1g} modes, respectively.

was observed in the 1:1 ordered pure BZT sample without B_2O_3 sintered at 1650 °C. The value of $Q \times f$ decreased as the degree of 1:2 ordering increased. Based on the results, it can be concluded that the increased $Q \times f$ value cannot be explained simply in terms of the 1:2 ordering. Davies et al.[10] reported that the improvement in the Q values in the 1:1 ordered $Ba(Zn_{1/3}Ta_{2/3})O_3$–$BaZrO_3$ system is caused by the

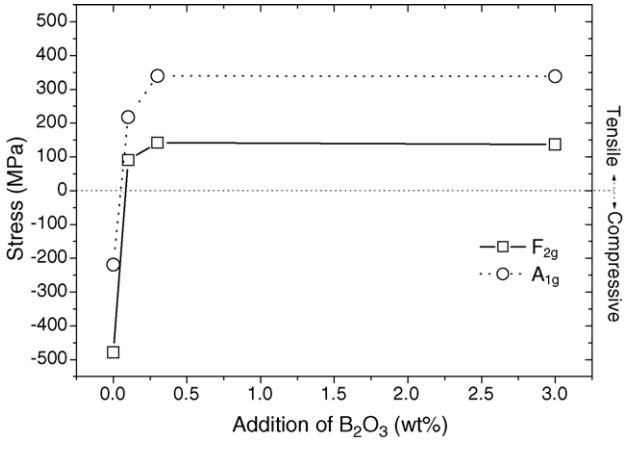

Fig. 7. Residual stress caused by lattice distortion as a function of the B_2O_3 content, as analyzed using the F_{2g} and A_{1g} modes.

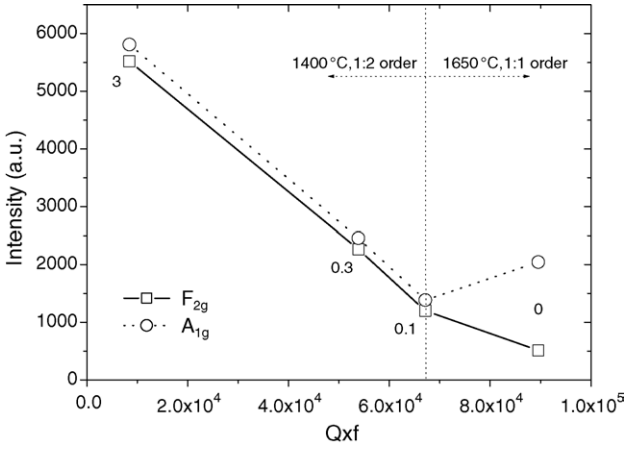

Fig. 8. Intensity changes of the F_{2g} and A_{1g} modes as a function of the $Q \times f$ value.

stabilization of antiphase boundaries with a random layer. It is believed that in the present system too, the high $Q \times f$ value can be attributed to the variation of the antiphase boundary, resulting from the replacement of the 1:2 ordering by 1:1 ordering, while the decrease in the $Q \times f$ value with increasing degree of 1:2 ordering can be attributed to the presence of a liquid phase whose amount increased with increasing B_2O_3 content.

5. Conclusion

The ordering and lattice distortion related to cation ordering in the $Ba(Zn_{1/3}Ta_{2/3})O_3$–B_2O_3 system were investigated using XRD and Raman spectroscopy. The 1:2 ordered structure of the pure BZT ceramic was replaced by a 1:1 ordered structure at 1650 °C. The addition of B_2O_3 improved the ordering in the BZT ceramics. The degree of 1:2 ordering increased with increasing B_2O_3 content. The Raman lines of the 1:1 ordered structure were shifted towards lower wavenumbers, as compared to those of the disordered structure. Thus, it was concluded that the 1:1 ordered ceramics were subjected to compressive residual stress. In the case of the 1:2 ordered structure, the Raman lines shifted towards higher wavenumbers, thus indicating that the lattice was subjected to tensile residual stress. The maximum $Q \times f$ value was obtained for the 1:1 ordered structure of the BZT ceramics sintered at 1650 °C. The value of $Q \times f$ decreased with increasing B_2O_3 content, in spite of the presence of a highly ordered 1:2 structure.

Acknowledgment

This work was supported by Korea Research Foundation Grant (KRF-2000-E00118) and we appreciated the partial support from the Venture Laboratory at Kyoto Institute of Technology.

References

1. Wersing, W., High frequency ceramic dielectrics and their application for microwave component. In *Electric Ceramics*, ed. B. C. H. Steels. Elsevier Applied Science, London, UK, 1991, pp. 67–119.
2. Moulson, A. J. and Herbert, J. M., *Electroceramics*. Chapman and Hall, London, UK, 1990, Chapter 5.
3. Nomura, S., Yoyama, K. and Kaneta, K., $Ba(Mg_{1/3}Ta_{2/3})O_3$ ceramics with temperature stable high dielectric constant and low microwave loss. *Jpn. J. Appl. Phys.*, 1982, **21**, 624.
4. Kawashima, S., Nishida, M., Ueda, I. and Ouchi, H., $Ba(Zn_{1/3}Ta_{2/3})O_3$ Ceramics with Low Dielectric Loss at Microwave Frequencies. *J. Am. Ceram. Soc.*, 1983, **66**(6), 421–423.
5. Tamura, H., Konoike, T., Sakabe, Y. and Wakino, K., Improved high-Q dielectric resonator with complex perovskite structure. *J. Am. Ceram. Soc.*, 1984, **67**, C59–C61.
6. Desu, S. B. and O'Bryan, H. M., Microwave loss quality of $Ba(Zn_{1/3}Ta_{2/3})O_3$ Ceramics. *J. Am. Ceram. Soc.*, 1985, **68**(10), 546–551.
7. Galasso, F., *Perovskite and High-T_c Superconductors*. Gordon and Breach, New York, 1990, pp. 3–72.
8. Jacobson, A. J., Collins, B. M. and Fender, B. E. F., A powder neutron and X-ray diffraction determination of the structure of $Ba_3Ta_2AnO_9$: an investigation of perovskite phases in the system Ba-Ta-Zn-O and the preparation of $Ba_2TaCdO_{5.5}$ and $Ba_2CeInO_{5.5}$. *Acta Crystallogr.*, 1976, **B32**, 1083–1087.
9. Matsumoto, K., Hiuga, T., Takada, K. and Ichimura, H., $Ba(Zn_{1/3}Ta_{2/3})O_3$ ceramics with ultralow loss at microwave frequencies. In *Proceedings of the 6th IEEE International Symposium on Application of Ferroelectrics (June 1986)*. Institute of Electrical and Electronics Engineers, New York, 1986, pp. 118–121.
10. Davies, P. K. and Tong, J., Effect of ordering-induced domain boundaries on low-loss $Ba(Zn_{1/3}Ta_{2/3})O_3$-$BaZrO_3$ perovskite microwave dielectrics. *J. Am. Ceram. Soc.*, 1997, **80**(7), 1727–1740.
11. Webb, S. J., Breeze, J., Scott, R. I., Cannell, D. S., Iddles, D. M. and Alford, N. M., Raman spectroscopic study of gallium-doped $Ba(Zn_{1/3}Ta_{2/3})O_3$. *J. Am. Ceram. Soc.*, 2002, **85**(7), 1753–1756.
12. Siny, I. J., Tao, R., Katiyar, R. S., Guo, R. and Bhalla A. S., Raman spectroscopy of Mg-Ta order-disorder in $Ba(Zn_{1/3}Ta_{2/3})O_3$. *J. Phys. Chem. Solids*, 1998, **59**(2), 181–195.
13. Lines, M. E. and Glass, A. M., *Principles and Applications of Ferroelectrics and Related Materials*. Clarendon, Oxford, 1977.
14. Smolensky, G. A., Siny, I. G., Pisarev, R. V. and Kuzrninov, E. G., *Ferroelectrics*, 1976, **12**, 135.
15. Galasso, F. F., *Structure Properties and Preparation of Perovskite Type Compounds*. Pergamon Press, London, 1969.
16. Kim, I.-T., Oh, T.-S. and Kim, Y.-H., Lattice distortion of $Ba(Zn_{1/3}Ta_{2/3})O_3$ with ordering of B-site cations. *J. Mater. Soc. Lett.*, 1993, **12**, 182–184.
17. Reaney, I. M., Qazi, I. Q. and Lee, W. E., Order-disorder behavior in $Ba(Zn_{1/3}Ta_{2/3})O_3$. *J. Appl. Phys.*, 2000, **88**(11), 6708–6714.
18. Pezzotti, G., In situ study of fracture mechanisms in advanced ceramics using fluorescence and Raman microprobe spectroscopy. *J. Raman Spectrosc.*, 1999, **30**, 867–875.